PHYSICAL REVIEW B VOLUME 27, NUMBER 3 1 FEBRUARY 1983

Interpretation of anomalies in the Raman spectrum of K_2SeO_4 in terms of oxygen sublattice disorder

Nestor E. Massa
Behlen Laboratory of Physics, University of Nebraska, Lincoln, Nebraska 68588

Frank G. Ullman
Behlen Laboratory of Physics and Department of Electrical Engineering, University of Nebraska, Lincoln, Nebraska 68588

J. R. Hardy
Behlen Laboratory of Physics, University of Nebraska, Lincoln, Nebraska 68588

(Received 29 December 1981; revised manuscript received 25 May 1982)

Raman scattering from K_2SeO_4 crystals has been studied in the (20—800)-K temperature range. Three portions of the spectrum are discussed: defect-induced scattering, primarily below 100 cm^{-1}, the external mode spectrum below 200 cm^{-1}, and the internal mode spectra in two regions, 300—500 and 800—950 cm^{-1}. The temperature dependence of the low-frequency, defect-induced scattering has been correlated (in previous studies) with the temperature dependence of certain nonzero-wave-vector phonons that have been observed by others using inelastic neutron scattering. Close to the incommensurate transition temperature, $T_i = 129$ K, a large enhancement and line narrowing develops below 10 cm^{-1}; no satisfactory interpretation of this effect has yet emerged. Above 129 K, in the paraelectric phase, the multiplicity of the external modes agrees with the predictions of the Raman-scattering selection rules. The internal mode spectra, however, consistently contain more lines than prescribed by the selection rules. These observed internal mode spectra would have the correct multiplicity if the crystal did not possess the center of symmetry of the presumed *Pnam* space group, thus suggesting a distortion of the selenate sublattice. Small frequency shifts above 375 K in the external mode spectra are similar to those observed in the incommensurate phase and, also, differential thermal analyses of powders and crystals show small, diffuse, reproducible peaks in the (373—473)-K range. Both effects may be associated with glasslike phase changes in the selenate sublattice. A qualitative model of orientational disorder in the selenate sublattice is offered to account for all these observations.

I. INTRODUCTION

Potassium selenate, K_2SeO_4, exhibits a number of phase-transition phenomena that have made it a subject of several recent investigations[1—8] (the references cited are representative, not all inclusive).

In this article, we describe a detailed study of the Raman spectrum of K_2SeO_4. Raman scattering is now a widely accepted technique for detecting Raman-active lattice-dynamical instabilities (phonons) associated with structural phase transitions in solids. Many investigators have used the technique to single out one or more of such unstable phonons and have then concentrated on studying their particular behavior resulting from variation of a variety of parameters. Such investigations have been fruitful in elucidating the nature of these unstable phonons. However, other important and relevant properties can be detected by studying the remainder of the spectrum. We show, in this paper, that from a study of the complete Raman spectrum of K_2SeO_4 [from 6 to 1000 cm^{-1} and in the (20—800)-K temperature range], several properties associated with the structural phase transitions in this material have been discovered.

Initially, the study of the complete spectrum was undertaken to check the first reports[2—4] of the Raman spectrum of K_2SeO_4 and to determine the frequencies of the allowed Raman-active phonons that were needed as initial parameters for lattice-dynamical calculations of the structural instability.[1] It became apparent that there were internal incon-

sistencies in our results as well as inconsistencies in their agreement with the results of others and also with the predictions of the selection rules. Consequently, more detailed studies were carried out to clarify this apparent confusion. The source of the confusion has proved to be more subtle and more complex than was first envisioned. We show here that K_2SeO_4 crystals, grown by slow evaporation of aqueous solutions, contain intrinsic defects, not observed by x-ray or neutron diffraction, but which influence the Raman spectra, particularly those of the internal modes.

In the following, the spectrum is divided into three parts: (1) a low- frequency region below 100 cm^{-1}, produced by defect-induced scattering, (2) the external mode spectrum below 200 cm^{-1}, and (3) the internal mode spectra in the frequency ranges 300—500 and 800—950 cm^{-1}. Each of these spectral regions is discussed separately below.

At this point, to ensure clarity in the remainder of this paper, it is necessary to cite certain relevant properties of K_2SeO_4 (a concise and thorough summary has been given recently by Petzelt *et al.*[7]). K_2SeO_4 has been reported to exist in four distinct phases: Phase 1 (above 745 K) is hexagonal, phase 2 ($129 < T < 745$ K) is orthorhombic ($Pnam$-D_{2h}^{16}), phase 3 ($93 < T < 129$ K) is incommensurate, and phase 4 ($T < 93$ K) is ferroelectric with an orthorhombic cell ($Pnam2_1$-C_{2v}^9) that has tripled along the a axis relative to phase 2. (Recent specific-heat measurements[9] show these Kelvin temperatures to be 734 ± 5 [differential-scanning-calorimetry (DSC) measurement], 128.6 ± 0.05, and 94.15 ± 0.05. Another weak transition was also found at 56.03 ± 0.05.) The temperatures at which transitions occur from phase 2 to phase 3 and from phase 3 to phase 4, respectively, are designated T_i and T_c. The transition at T_i is continuous, whereas the one at T_c is weakly first order. Although a dielectric anomaly is observed at T_c, several other properties behave normally at T_c but anomalously at T_i (e.g., thermal expansion, ESR response, and the decrease to zero of the soft-mode frequency in phases 3 and 4), which is now known to be the temperature of an incommensurate transition caused by the softening of a Σ_2 mode in phase 2 with a wave vector of $(a^*/3)(1-\delta)$ in phase 3. (a^* is the reciprocal of the a axis length multiplied by 2π, and δ is a temperature-dependent quantity that decreases from about 0.07 at T_i to zero on cooling to T_c.[5]) The fact that these changes in physical properties originate from an incommensurate structural phase transition is mainly responsible for the interest in this material.

II. EXPERIMENTAL DETAILS

A. Sample preparation

K_2SeO_4 crystals were prepared by slow evaporation, at room temperature and at 50 °C, from aqueous solutions of 99.9%-pure Alfa Products powder. The crystals were oriented by x-ray diffraction and were usually polished into right-angle-sided prisms with the sides parallel to the orthorhombic crystallographic axes. (A 45° geometry was also used for one set of measurements as discussed below.)

B. Apparatus

The light-scattering system has been described previously.[10] All measurements were made with either the 488- or 514.5-nm argon-ion laser line with fixed-time photon counting in 0.5-nm steps; the same results were obtained with both wavelengths. The spectral resolution was about ±1.5 cm^{-1}, and all spectra were calibrated against selected neon lines. All data were stored on floppy disks and subsequently plotted on a digital x-y recorder. Several different sample cells were used in this work; all except the low-temperature, helium-gas flow Dewar[11] were of standard design. Differential-thermal-analysis (DTA) measurements were made on a Columbia Scientific Industries, model DTA-200 system in an inert atmosphere (see Acknowledgments).

C. *Designation of scattering configurations*

Although all investigators now use the standard notation [incident and scattered *polarizations* enclosed in parentheses and incident and scattered *propagation directions* on the left- and right-hand sides of the parentheses, respectively, e.g., $x(zx)y$], Raman-scattering spectra from K_2SeO_4 have been assigned different symmetries in different publications because the authors assign different Cartesian axes (x,y,z) to the *crystal* axes (a,b,c). We have avoided this confusion by writing all scattering configurations in terms of the orthorhombic crystal axes $c < a < b$ ($a=7.661\pm0.004$ Å, $b=10.466\pm0.008$ Å, and $c=6.003\pm0.003$ Å). We have used the notation of Refs. 1 and 5 in which the axes x, y, and z correspond to a, b, and c, respectively, for the assignment of irreducible representations to given scattering configurations. These and the choices of others[2–4] are summarized in Table I. All are

TABLE I. Assignments of Cartesian axes to crystal axes in the references indicated.

	Iizumi *et al.*,[a] Haque and Hardy,[b] in this paper	Wada *et al.*[c]	Fawcett *et al.*[d]	Caville *et al.*[e]
x	a	c	a	c
y	b	b	c	a
z	c	a	b	b

[a]Reference 5.
[b]Reference 1.
[c]Reference 4.
[d]Reference 2.
[e]Reference 3.

correct since the choice of Cartesian axes is arbitrary.

If the symmetry designations for the Raman-active modes are chosen to conform with the *Pnam* space group, the corresponding polarizability matrices are as follows:

$$\begin{bmatrix} aa & & \\ & bb & \\ & & cc \end{bmatrix}, \quad A_g \qquad \begin{bmatrix} & ab & \\ ba & & \\ & & \end{bmatrix}, \quad B_{1g}$$

$$\begin{bmatrix} & & ac \\ & & \\ ca & & \end{bmatrix}, \quad B_{2g} \qquad \begin{bmatrix} & & \\ & & bc \\ cb & & \end{bmatrix}. \quad B_{3g}$$

This is consistent with the symmetry classification in Refs. 1 and 5.

III. EXPERIMENTAL RESULTS

A. The low-frequency band

A preliminary report on this band has already been published.[6] In early measurements, it is noted that many of the spectra, in all scattering configurations, had a small shoulder below 50 cm^{-1} on the rapidly changing, unshifted background. Later, when attempting to maximize the signal-to-background ratio by varying the position of the focus of the incident light in the crystal, this shoulder became a resolved band of about 50-cm^{-1} halfwidth and with a count comparable to the strongest external modes. It can be seen in all scattering configurations but is best resolved for $a(cc)b$. (The crystal axes were incorrectly identified in Ref. 6.) An example at room temperature is shown in Fig. 1. The small amplitude fluctuations superposed on the band are greater in intensity than the noise and thus are genuine, as can be seen from a comparison with the noise on the background at higher wave numbers. The line shape of this band changes markedly with temperature (both above and below 295 K); a few typical curves for $T > 300$ K are shown in Fig. 2. Below 300 K, there is a general downshift in peak frequency but no drastic change until the sample temperature is close to T_i. At this temperature, a sharp peak appears below 10 cm^{-1} of more than an order of magnitude greater intensity than the rest of the band, as shown in Fig. 3. A few degrees below T_i, this disappears but the broad band persists to temperatures below 77 K. Its detailed behavior, however, appears to be specimen dependent.

The band just described could be a consequence of defect-induced scattering and thus would be some weighted mapping of the phonon density of states. However, because its intensity is comparable

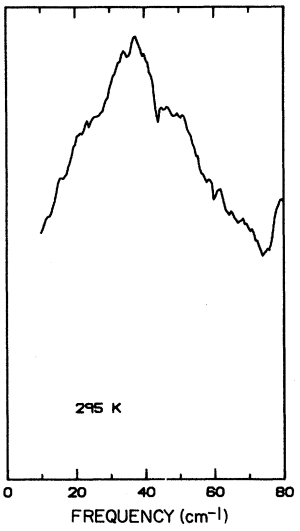

FIG. 1. Raman spectrum of the defect-induced band at 295 K, 488-nm excitation.

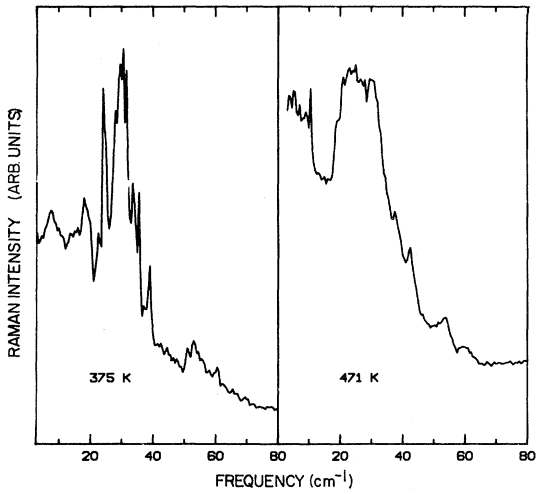

FIG. 2. Examples of the spectrum of the defect-induced band at two other temperatures, 375 and 471 K, 488-nm excitation.

to the external mode intensities, the defect concentration must be large. Proceeding on the assumption that this band is defect induced and thus contains contributions for all of the phonons rather than just the zone-center phonons responsible for Raman scattering from more perfect crystals, three features of the band, at which inflections appeared to occur, were selected and their frequencies followed as a function of temperature. As we have reported previously,[6] the observed temperature dependence of each of these frequencies can be shown to be the same as that observed by neutron scattering[5]

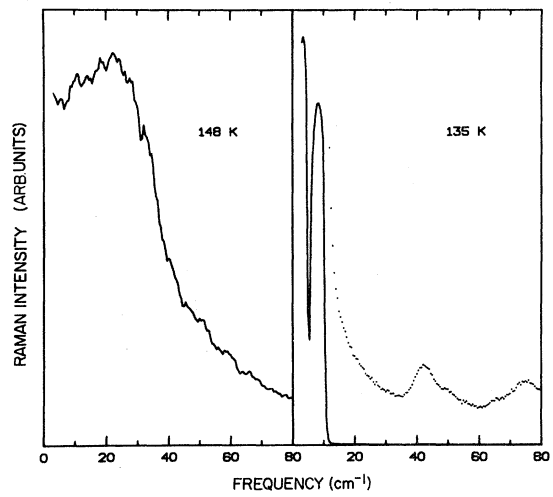

FIG. 3. Enhancement of the defect-induced band at 135 K and for comparison, the same band at 148 K. The dotted curve for 135 K is the solid curve magnified 90 times, 488-nm excitation.

for the nonzero wave vector, soft phonon, and the zone-center and/or zone-boundary phonon on the same branch. This result provides strong support for the hypothesis that this band arises from defect-induced scattering.

Next, the problem of identifying the defect(s) responsible for this low-frequency scattering was addressed. A number of mixed crystals were prepared, with additions of Rb, Cs, or Na, to determine if intrinsic or extrinsic defects were involved.[12] No essential differences in this low-frequency band were observed; thus it was concluded that the defects were *intrinsic*. Since the experiments to be described in the next section give an indication of the nature of these intrinsic defects, further discussion is deferred to a later section.

B. Modal analysis

In phase 2, potassium selenate apparently possesses the β-K_2SO_4 structure (see Ref. 1 for details), in which there are four molecules in the crystallographic cell. ($\underline{K_2SO_4}$ is underlined wherever it occurs to avoid confusion with K_2SeO_4.) Thus, 81 optic modes are possible. From point-group analysis, these are subdivided as tabulated in Table II. Below 143 K, $\underline{K_2SO_4}$ belongs to the space group C_{2v}^9 ($Pnam2_1$) as does K_2SeO_4 below 93 K, except that in $\underline{K_2SO_4}$ there is no change in cell dimensions on cooling through 143 K. In K_2SeO_4, the cell triples in the a direction below 93 K so in this phase, it will have 3 times as many modes as $\underline{K_2SO_4}$. The modal analysis for this low-temperature phase of $\underline{K_2SO_4}$ is given in Table III.

For the β-$\underline{K_2SO_4}$ phase of K_2SeO_4, since only the

TABLE II. Vibrational mode assignments for the β-$\underline{K_2SO_4}$ (D_{2h}^{16}) structure (paraelectric K_2SeO_4) (T=translational, L=librational).

Mode assignment	Number of internal modes	Number of external modes T	L
$A_g(aa,bb,cc)$	6	6	1
$B_{1g}(ab)$	6	6	1
$B_{2g}(ac)$	3	3	2
$B_{3g}(bc)$	3	3	2
A_u	3	3	2
B_{1u}	3	2	2
B_{2u}	6	5	1
B_{3u}	6	5	1

TABLE III. Vibrational mode assignments for the low-temperature phase ($T < 143$ K) of $\underline{K_2SO_4}$ which has point symmetry C_{2v}^9.

Mode assignment	Number of internal modes	Number of external modes
A_1	9	11
A_2	9	12
B_1	9	11
B_2	9	11

gerade modes are Raman active, we should expect to see four distinct sets of spectra for scattering configurations corresponding to each of the symmetry groups, A_g, B_{1g}, B_{2g}, and B_{3g}. The analysis of the spectra that follows is made with these assignments in mind as described in Tables II and III.

C. The external mode spectrum in phase 2

In this phase, the crystal is paraelectric and has at least one incommensurate soft mode. To obtain sufficient resolution to observe the predicted number of modes, it was necessary to cool below room temperature. The observed lines are listed in Table IV and typical spectra measured at about 140 K are shown in Figs. 4 and 5. In these and all subsequent spectra and tabulations we show data for two different specimens: We do this in light of the specimen dependence referred to later.

The number of lines in Table IV for each symmetry group conforms to the predictions of the selection rules; the few extra lines that are observable are weak and, as discussed later, could be expected. There is general agreement between the results of Wada *et al.*[4] and ours for these external modes.

As stated above, these results show the external modes of the crystal in the paraelectric phase, in the range from T_i up to room temperature, to be as predicted by the selection rules for the $\underline{\beta\text{-}K_2SO_4}$ structure. The spectra for temperatures below T_i are more complex but are not needed to support the model to be presented later, and for these reasons, they are not included in this paper.

D. The internal mode spectra

Except for thermal broadening, these spectra remain essentially the same in all four phases. The free selenate ion is tetrahedral and thus has four distinct vibrational frequencies (a nondegenerate A_1 mode, a doubly degenerate E-type mode, and two triply degenerate F_2-type modes). The correlation table for these modes and the Raman-active modes in phase 2 of K_2SeO_4 ($Pnam$-D_{2h}^{16}) is given in Table V. The internal modes fall in two spectral regions. Lines derived from ν_2 and ν_4 (the bending modes) lie in the (300—500)-cm^{-1} range and lines derived from ν_1 and ν_3 (the stretching modes) lie in the (800—950)-cm^{-1} range. For convenience, these two ranges are designated as the "bending" and "stretching" regions, respectively, and Table V can be used to determine the distribution of lines between these two regions of the internal mode spectrum. For example, the A_g spectrum should have three lines in the bending region and three in the stretching region, whereas the B_{2g} spectrum should have two in the bending region and just one in the stretching region. In Figs. 6—9, internal mode spectra for each symmetry, separated into the two spectral regions, are shown. In Table VI, both the measured intensities and the intensities relative to the strongest line in each spectrum are listed.

Although these spectra are qualitatively similar to those reported by others,[2—4] they exhibit several important quantitative differences. The main difference lies in whether or not a strong line at about 840 cm^{-1} appears with high relative intensity in all of the spectra. Also, extra lines appear in

TABLE IV. Observed lattice mode frequencies of potassium selenate for two crystals. Question marks denote questionable values.

Polarization	*aa*		*bb*		*cc*		*ab*		*ac*		*bc*	
Crystal	1	2	1	2	1	2	1	2	1	2	1	2
			45	37	40—50	47?	50?	45?	48	52	45	44
	75	75	75	75	75	78	73	75	75	75	75	75
	95	98	97	95	97	98	95	97	95	96	95	92
	105	105	105	105	105	105	105	105?				
		120	120	125	120	120		120?	118	120	118	121
	145	144	144			145	140?	143	146	145—150	140	144
	162	162					160?	160				

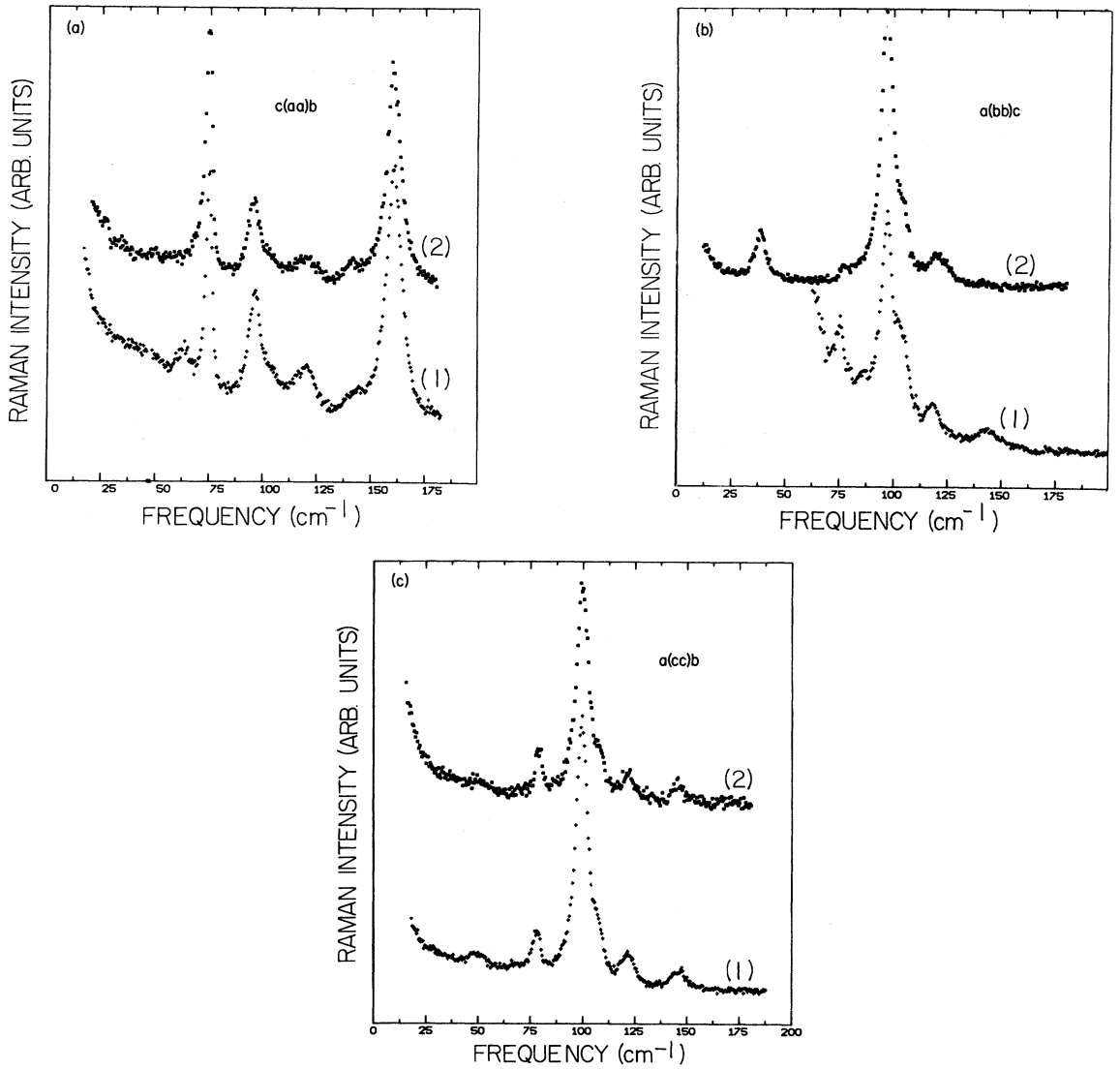

FIG. 4. Lattice mode spectra of the A_g modes for two crystals. (a) $c(aa)b$, (b) $a(bb)c$, (c) $a(cc)b$.

each spectrum with about 10% of the relative intensity of the strongest line. These have either been ignored or written off as "polarization leakage" in the references cited although no justification for such an interpretation has been offered. Our results indicate that the appearance of the 840-cm^{-1} line with large intensity in any but the diagonally polarized [(*aa*), (*bb*), or (*cc*)] spectra is caused either by twinning [many crystals grow as 60° twins in the *bc* plane as in the aragonite form of $CaCO_3$ (Ref. 13)] or by some unidentified physical damage from existing internal stress or temperature cycling through the 93-K transition. The 840-cm^{-1} line is allowed in the (*ab*) spectrum but only because principal polarizability axes of the SeO_4 groups are not aligned with the *a* and *b* axes of the crystal, whereas one such axis is parallel to the *c* direction, so even in (*ab*) spectra, its relative intensity should not be large.

All of the published work to date[2–4] shows the 840-cm^{-1} line to be the strongest in cross-polarized spectra. By selecting untwinned crystals, we have obtained cross-polarized spectra with relatively weak 840-cm^{-1} lines.

We have also observed that the 840-cm^{-1} line intensity in a given spectrum may increase after cooling the crystal below 93 K and reheating. Since the crystals are known to experience thermal shock and eventual cracking from such temperature cycling, we believe that perhaps, some physical damage oc-

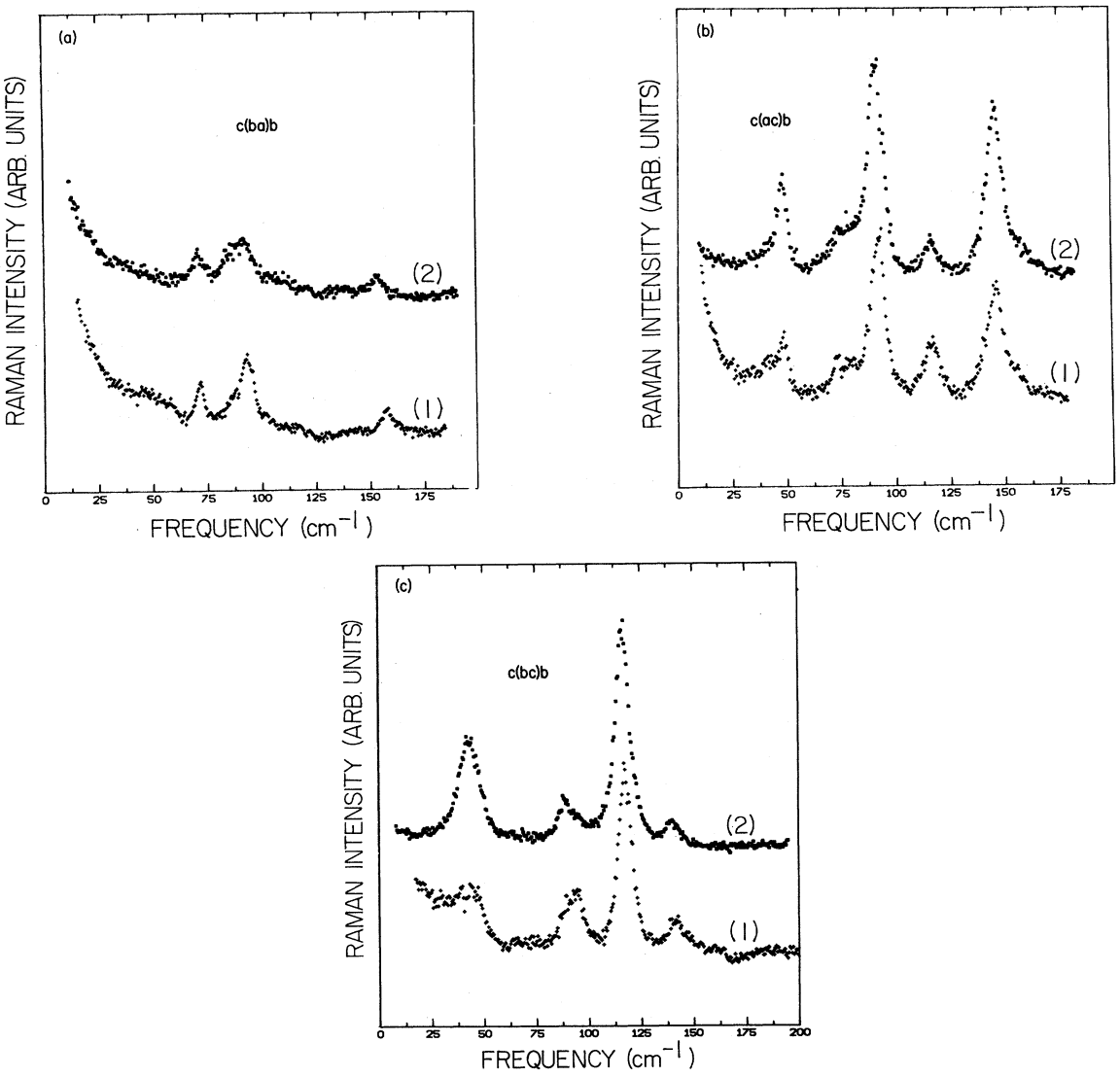

FIG. 5. Lattice mode spectra of the B_{1g}, B_{2g}, and B_{3g} modes for two crystals. (a) $c(ba)b$, (b) $c(ac)b$, (c) $c(bc)b$.

curs that can give rise to small cracks or misoriented regions and concomitant depolarization. Examples of these differences are shown in Figs. 8 and 9.

It can be seen in Figs. 6—9 that in addition to the strong "allowed" lines, other lines appear in all the spectra with lower intensity so that the same nine lines appear in each of the internal mode spectra, for each irreducible representation, rather than the number predicted by the selection rules and shown in Table II. It is always possible that the weaker lines can be attributed to "polarization leakage" from polarizations in which they appear with high relative intensity, since K_2SeO_4 is biaxial and the incident and scattered light are convergent and diver-

TABLE V. Correlation table for the internal modes of potassium selenate.

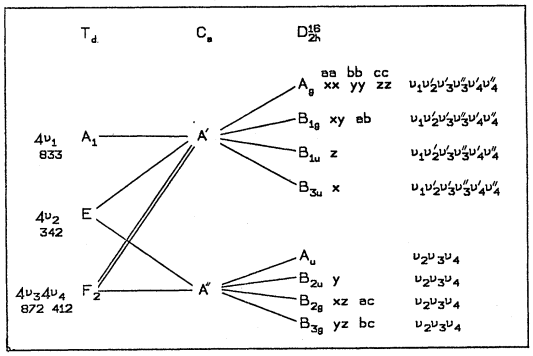

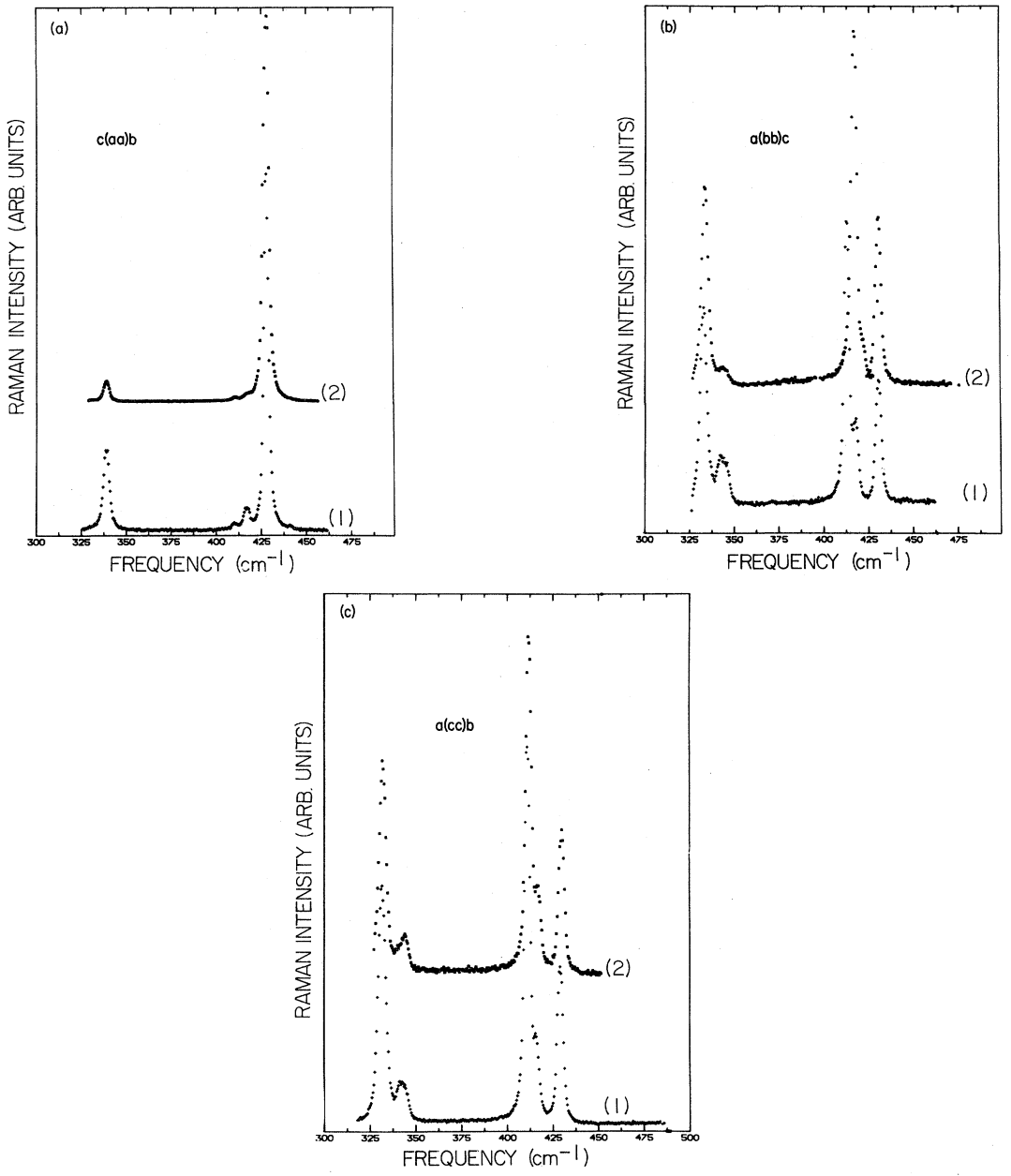

FIG. 6. A_g modes in the bending region for two crystals. (a) $c(aa)b$, (b) $a(bb)c$, (c) $a(cc)b$.

gent, respectively. When the lens that focuses the incident light into the sample was removed, no significant changes in the spectra were observed, so the convergent incident light did not produce significant depolarization effects. The depolarized content of the scattered light was also checked by comparing spectra for different aperture settings of the collecting lens over an f-stop range of 5.6 to 11, or a reduction of the collection angle by about $\frac{1}{2}$. Although in some of the cross-polarized spectra, this reduced the relative intensity of the 840-cm^{-1} line, in no case was the reduction great enough to suggest that the presence of all of the weaker "forbidden" lines could be attributed to leakage. Also, the relative intensities of the weaker lines vary from sample to sample, indicating a specimen dependence. Thus we concluded that in the qualitative analysis of the spectra given here, all of the lines reported can be assumed to belong to the spectrum in which they are observed.

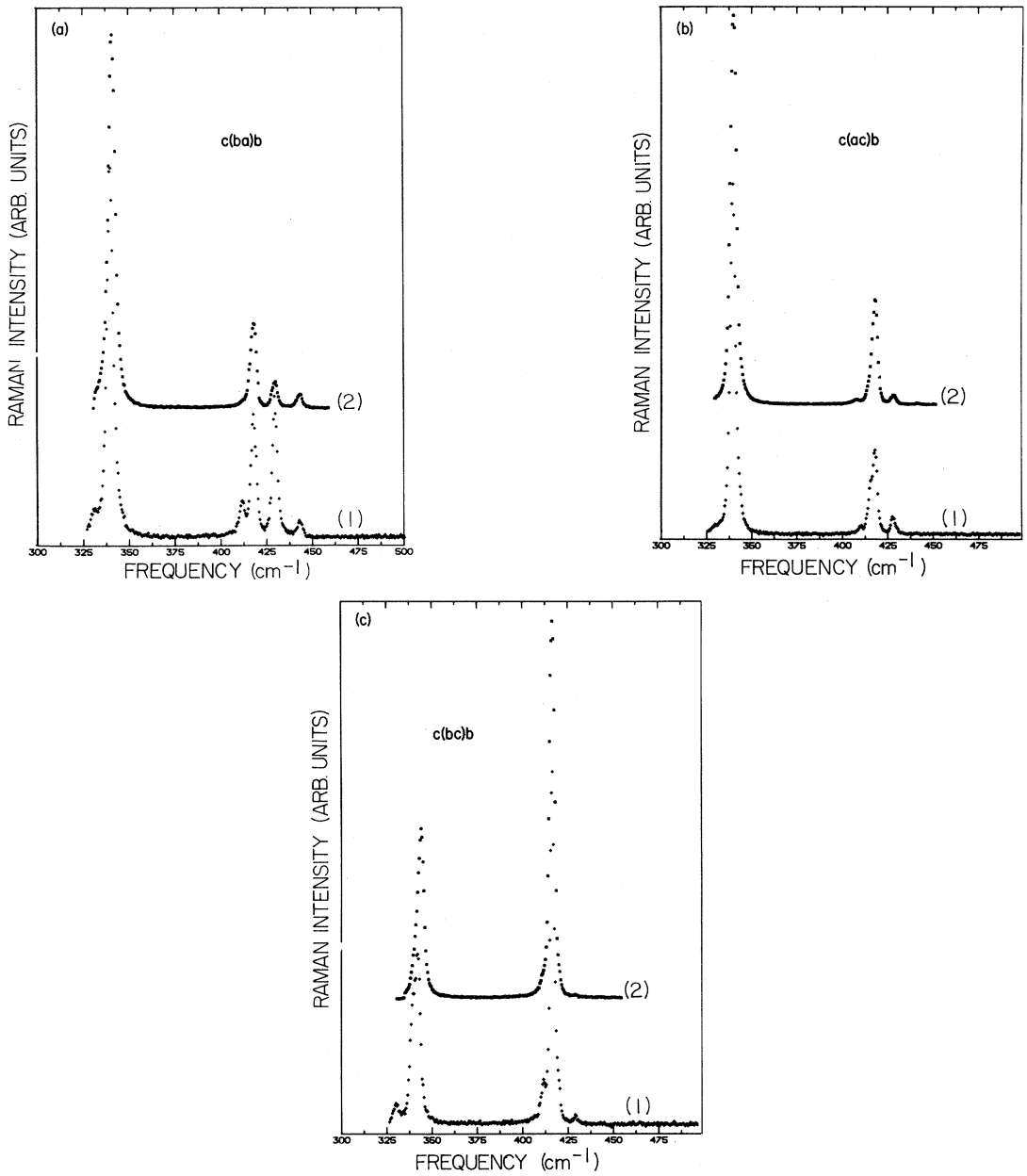

FIG. 7. B_{1g}, B_{2g}, and B_{3g} modes in the bending region for two crystals. (a) $c(ba)b$, (b) $c(ac)b$, (c) $c(bc)b$.

This disagreement with the predicted multiplicity was puzzling at first. It was noted, however, that β-K_2SO_4, which is isomorphous with phase 2 of K_2SeO_4, undergoes a phase transition on cooling in which the center of inversion of the β phase is destroyed. The predicted numbers of internal modes for this noncentrosymmetric phase are nine for each symmetry, as described earlier and shown in Table III. This suggested that our K_2SeO_4 crystals, although seemingly of high perfection and of *Pnam* symmetry in phase 2 from x-ray diffraction,[14] might not appear centrosymmetric to a Raman probe. (This is not a new idea; it has been offered before to explain similar anomalies in Raman spectra.[15,16])

Examination of the spectra suggests the "allowed" lines should be identified as those that are strongest and of a number corresponding to the selection rule predictions as shown in Table VII. The additional lines are those in excess of the pre-

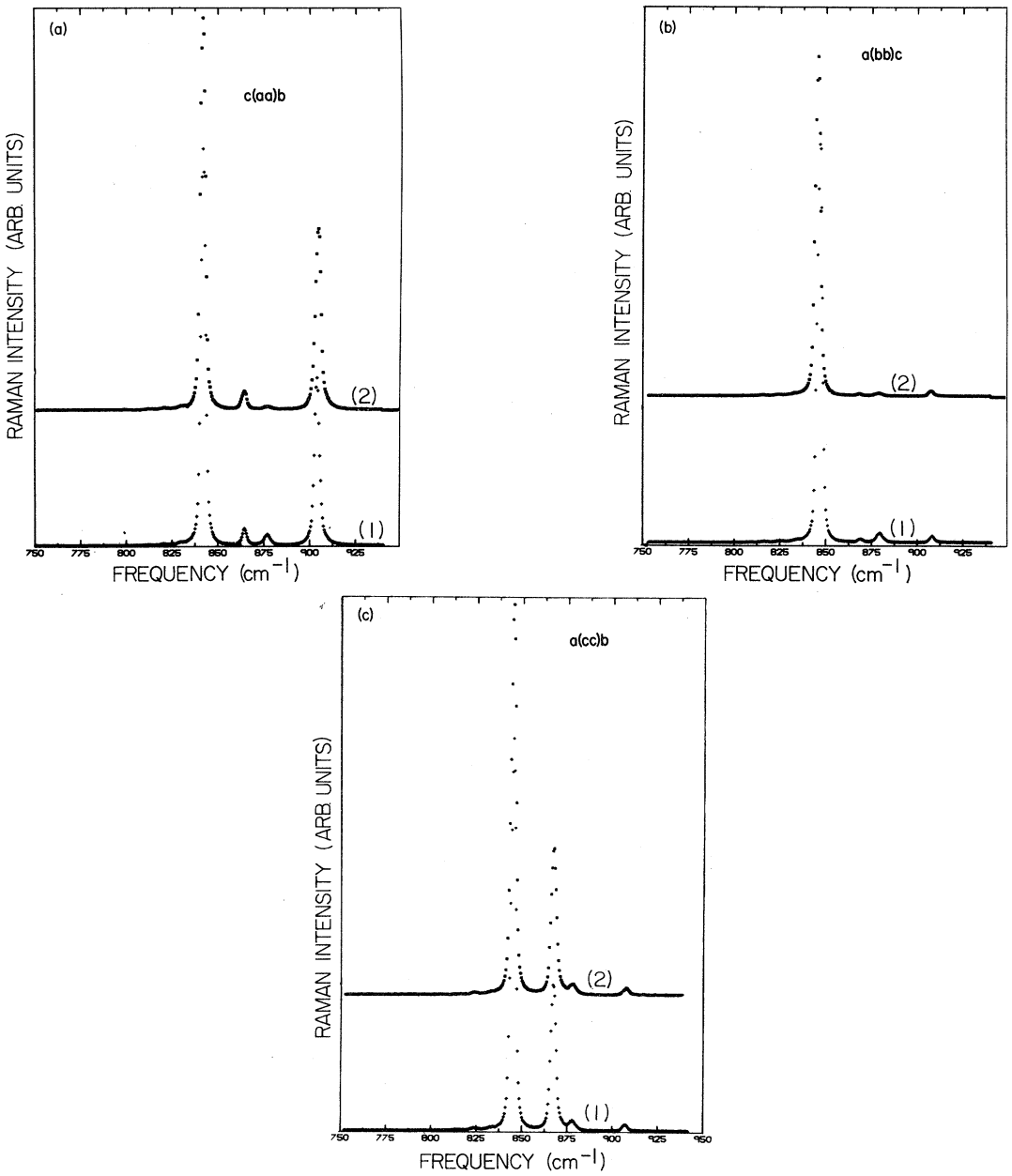

FIG. 8. A_g modes in the stretching region for two crystals. (a) $c(aa)b$, (b) $a(bb)c$, (c) $a(cc)b$.

dictions of the selection rules; these are shown in parentheses in the table.

Finally, if the paraelectric phase did have the β-K_2SO_4 structure, then it could be argued that the relatively low-intensity extra lines in each spectrum became observable from depolarization effects (leakage). However, if this were the case, below 93 K there should be 36 Raman-active lines times 3, because of the cell tripling, 108 Raman lines in all. The theoretical calculations[1] showed many of the modes to have sufficient dispersion for this splitting to be observed. Since we see only the same nine lines in all symmetries at all temperatures, we must conclude that the internal modes do not obey the selection rules predicted for K_2SeO_4 and that all of the observed lines are genuine.

This departure of the internal mode spectra from predicted behavior, along with the observation of the defect-induced scattering that we have shown to be associated with intrinsic defects, supports a hy-

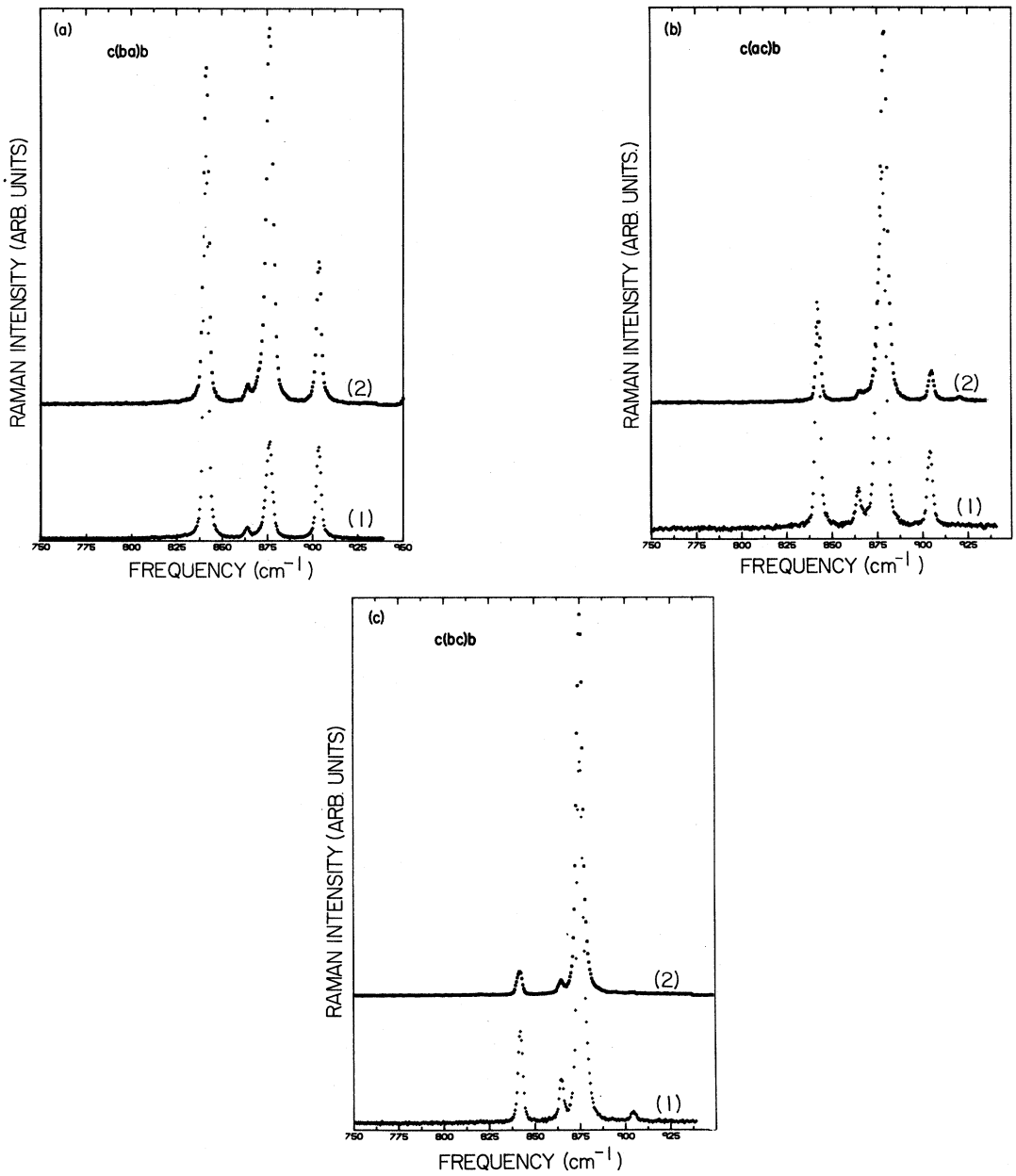

FIG. 9. B_{1g}, B_{2g}, and B_{3g} modes in the stretching region for two crystals. (a) $c(ba)b$, (b) $c(ac)b$, (c) $c(bc)b$.

pothesis that the defects are associated with the selenate sublattice and have destroyed its inversion symmetry. Since the external modes appear to satisfy the selection rules for D_{2h}^{16}, the potassium-ion sublattice is probably not involved significantly in this defect structure.

In addition to the experiments just described, measurements were also made on crystals with sides cut along {110} planes so that phonons propagating along the crystal axes could be studied. (In right-angle scattering measurements on {100}-cut crystals, the phonons propagate at 45° in the scattering plane.) Thus purely transverse or purely longitudinal polar phonons can be observed. If the selenate sublattice does not have a center of inversion, as postulated here, 27 of the 36 internal modes will be polar modes (C_{2v}^{9} symmetry). Since none of the modes of K_2SeO_4 is degenerate, the macroscopic field associated with longitudinal vibrations will not produce additional lines; for polar modes, however,

TABLE VI. (a) Peak photon counts for two crystals. Question marks denote questionable values. (b) Ratio of peak counts to that of strongest line in each spectrum.

Peak	*aa*		*bb*		*cc*		*ab*		*ac*		*bc*	
Frequency	1	2	1	2	1	2	1	2	1	2	1	2
						(a)						
333	186?	350	6 152	4 144	7 677	3 695	436	700	287?	882	361	116
343	1 925	2 227	2 107	656	1 566	985	4 381	12 867	6 803	33 482	2 110	7 617
414	288	615	8 518	5 298	12 008	5 638	517	409	263	566	638	?
419	625	1 074	3 107	1 194	3 047	1 741	1 522	2 997	1 143	9 007	4 246	16 778
430	8 208	38 749	4 166	3 560	5 137	2 613	1 732	1 015	1 700	939	225	292
844	54 826	32 652	120 540	91 118	46 830	54 104	17 405	10 734	2 668	3 128	1 667	1 843
865	2 503	1 684	2 065	996	17 482	20 596	606	820	567	555	849	1 231
875	1 695	423	3 799	1 156	1 383	1 975	4 471	11 978	4 132	13 946	6 222	27 582
906	23 247	15 135	2 959	1 760	896	1 447	4 234	4 601	978	1 298	308	321
						(b)						
333	0.023?	0.009	0.722	0.782	0.639	0.653	0.010	0.054	0.042?	0.026	0.085	0.007
343	0.230	0.057	0.247	0.124	0.130	0.175	1	1	1	1	0.497	0.454
414	0.035	0.016	1	1	1	1	0.118	0.032	0.039	0.017	0.150	?
419	0.076	0.028	0.365	0.225	0.254	0.309	0.347	0.233	0.168	0.269	1	1
430	1	1	0.489	0.672	0.428	0.463	0.395	0.079	0.250	0.028	0.053	0.017
844	1	1	1	1	1	1	1	0.896	0.646	0.224	0.268	0.067
865	0.046	0.052	0.017	0.011	0.372	0.381	0.035	0.068	0.137	0.040	0.136	0.045
875	0.031	0.013	0.032	0.013	0.030	0.037	0.257	1	1	1	1	1
906	0.424	0.464	0.025	0.019	0.019	0.027	0.243	0.384	0.237	0.093	0.050	0.012

TABLE VII. Classification of internal modes. Bars: strongest lines in most cases—selected as those predicted by selection rules. Vertical dots: extra lines seen in spectrum. Note: Some intensity reversals can be seen in Table VI that suggest other choices for line identification could be made; however, these can be attributed to leakage from a similar strong line [e.g., leakage from (*cc*) into (*aa*)].

Irreducible representation	Polarization	Frequency (cm^{-1})								
		333	343	414	419	430	844	865	875	906
A_g	*aa bb cc*	|	⋮	|	⋮	|	|	|	⋮	|
B_{1g}	*ab*	⋮	|	⋮	|	|	|	⋮	|	|
B_{2g}	*ac*	⋮	|	⋮	|	⋮	⋮	⋮	|	⋮
B_{3g}	*bc*	⋮	|	⋮	|	⋮	⋮	⋮	|	⋮

there can be an angular dependence of frequency as the phonon polarization is changed from purely transverse to purely longitudinal. No significant frequency shifts from those shown for {100}-cut crystals were observed in these experiments so any angular dependence of phonon frequency is less than about 2 cm^{-1}.

E. Experimental evidence for defect phases above T_i

In view of the results just described, it was necessary to reassess the structural information on K_2SeO_4. In phase 1, above 745 K, the crystal is hexagonal,[17] and the selenates are believed to be completely disordered between "up" and "down" orientations along the *a* axis.[18] Below 745 K, our results show the crystal to be noncentrosymmetric and thus, not of the *Pnam* space group symmetry indicated by x-ray diffraction.[19] However, our x-ray diffraction measurements[14] indicate a high degree of crystal perfection with *Pnam* symmetry. Thus, a defect structure must be present that is not detected by x-ray diffraction but is seen by Raman scattering.

So far, two experimental observations—the defect-induced band and the noncentrosymmetric internal mode spectra—have been cited as evidence for defects in the selenate sublattice that produce a lower symmetry than *Pnam*. A few other observations should also be cited. First, at temperatures above about 375 K, a fine structure appears on the defect-induced band in the form of small spikes that are well above the noise level. Second, measurements of the temperature dependence of some peak frequencies in the lattice region show small changes above T_i and also similar but smoother changes at temperatures above 375 K.

These observations led us to suspect the existence of other phase transitions above room temperature. Consequently, DTA measurements were undertaken. The results, shown in Fig. 10, consistently show diffuse peaks in the (375—500)-K region reminis-

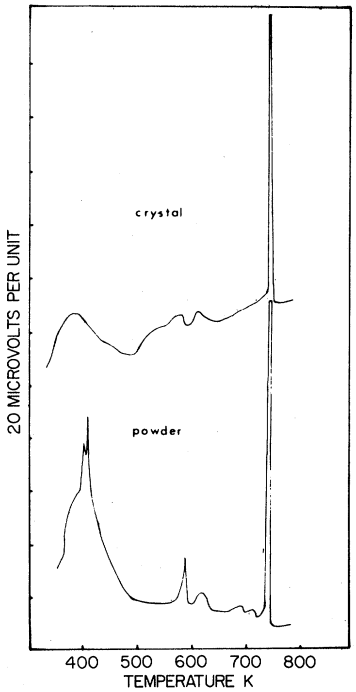

FIG. 10. DTA data for K_2SeO_4 crystal and for K_2SeO_4 powder.

cent of those associated with known glassy phase transitions. The sharper, and much larger peak at 745 K for the phase-1 to phase-2 transition is also shown for comparison. These "glassy" peaks could well be associated with a series of selenate rearrangements at various temperatures.

IV. TENTATIVE MODEL OF THE TRUE SELENATE STRUCTURE

The basic paradox that must be resolved is the apparent inconsistency between the x-ray structure and the results that have been described. The latter force us to the conclusions that "defects" must be present, that such defects are intrinsic, and that their concentration is large. As regards the last conclusion, the results suggest that each unit cell may be "defective." In Fig. 11, the structure obtained from our x-ray studies is shown; this is presented on the standard fashion (see figure caption) and shows the average atomic positions. The "thermal ellipsoids" that indicate the average excursions about each of these positions are also shown. This appears to be the centrosymmetric β-K_2SO_4 structure; however, it should be noted that the presence of a center of inversion symmetry is difficult to establish conclusively from x-ray studies. Specifically, for K_2SeO_4, while the potassium and selenium sublattices are probably centrosymmetric, the inversion symmetry of the oxygen sublattices is less certain. This is so because the total x-ray scattering is dominated by those contributions from atoms of high atomic number. However, it is also likely that if the average positions of the oxygen atoms from a regular sublattice of lower symmetry—specifically,

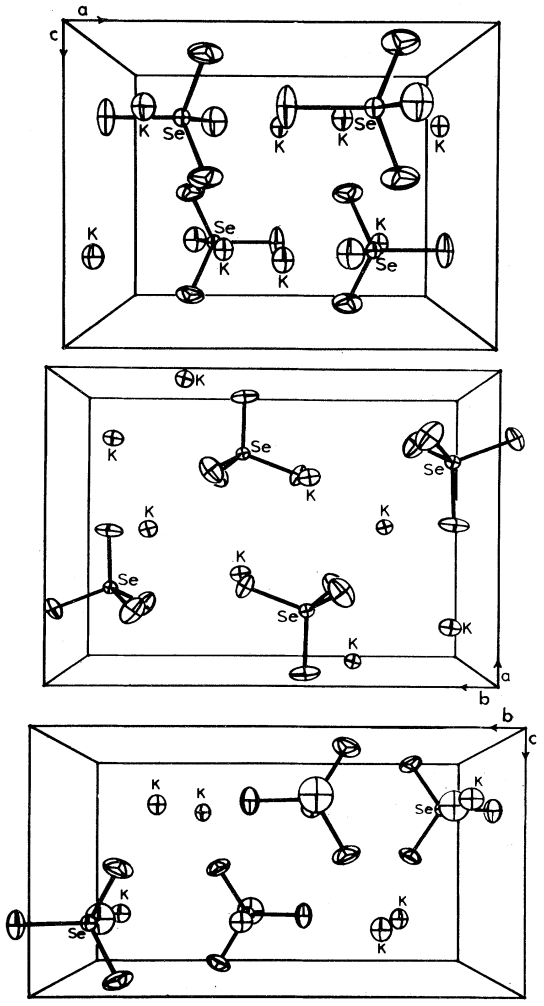

FIG. 11. ORTEP plots showing "thermal ellipsoids," from x-ray diffraction measurements of the K_2SeO_4 structure.

one lacking inversion symmetry—the x-ray diffraction would detect this fact. Moreover, while such a structure would be consistent with the Raman spectra observed at high and intermediate frequencies (the internal mode regions), it would also lead one to expect extra lines in the low-frequency external mode region. Since both gerade and ungerade modes of the centrosymmetric structure become Raman active when the center of inversion is lost, the total number of lines observed in the external mode region should be almost doubled (45 vs 24). Examination of the spectra reveals no such systematic near doubling, although a few additional lines of low intensity may be present in addition to the low-frequency band scattering discussed earlier and attributed to defects. Given the presence of such defects, additional lines may well be observed outside the defect-induced band in the low-frequency spectra; however, the number to be expected and their relative strengths are not predictable. As will be shown below, it is much easier to develop a model involving defects that is consistent with the fact that the numbers of observed Raman-active *external* modes are basically consistent with those predicted for the centrosymmetric (*Pnam*-D_{2h}^{16}) structure. There is certainly no evidence for scattering from all 21 additional modes that become Raman active when inversion symmetry is lost while translational symmetry remains. Moreover, the model developed below leads us to expect this behavior.

We thus return to the necessity of developing a model of K_2SeO_4 that predicts a structure with a high concentration of intrinsic defects, whose presence is not sensed by x-rays, and only slightly affects the Raman activity of the external (lattice) modes of the system while profoundly affecting the internal mode spectra. The only possibility that seems available is to hypothesize that the selenate tetrahedra are rotated, or canted, slightly away from their "ideal" locations in the β-K_2SO_4 structure. However, the motion involved is solely one of the oxygen ions. If the canting motions of different SeO_4 groups are essentially uncorrelated, or show only short-range correlation, then the average structure seen by x-rays will be that of β-K_2SO_4. However, the disordering of the selenates will manifest itself as an elongation of the "thermal ellipsoids" for the oxygen ions along the direction(s) of rotation. The structure shown in Fig. 11 (Ref. 14) is consistent with this interpretation.

This behavior of the selenates is easily explicable if it is assumed that the "ideal" positions of the oxygens correspond to local *maxima* in their potential energies which lie close to two (or more) minima which they can reach by relatively slight selenate rotations. This type of situation is similar to that which has been suggested to exist for the fluorine ions in the perovskite structure materials $KCaF_3$ (Ref. 20) and shown to exist for $RbCaF_3$ (Ref. 21); moreover, comparison of the thermal ellipsoids for the fluorine ions in Fig. 4(a) of Ref. 20 with those for the oxygen ions in Fig. 11 shows a suggestive similarity.

There is, however, one major difference between the situation for K_2SeO_4 and that for $KCaF_3$ and $RbCaF_3$; in the last two materials, the neighboring CaF_6 octahedra have one fluorine ion in common, whereas in K_2SeO_4 there is no such sharing of oxygen ions. This difference is crucial to our present model since we wish the selenate rotations to be only weakly correlated: a situation manifestly impossible if they are directly coupled by a shared oxygen ion, but not unreasonable in the β-K_2SO_4 structure where each is separate and surrounded by a loose "cage" of potassium ions.

This model is unusual in that it predicts the coexistence of a "glassy" oxygen sublattice lacking long-range order and a normal periodic structure for the other constituents. The crucial requirement for it to be valid is that the depths Δ of the potential minima for the selenates be significantly larger than any interselenate coupling. If this is the case, then when $kT \leq \Delta$, each selenate will begin to occupy one or the other of the local minima preferentially. However, there will be no long-range correlation between the rotations of *different* selenates since the coupling between them is much smaller than kT. Put more formally, one can say that the selenate sublattice can reduce its thermodynamic internal energy by selenate rotations into their respective potential minima without essentially changing its configurational entropy if there is no long-range correlation between the senses of rotation of pairs of selenates.

At lower temperatures, one expects the state of lowest free energy to have some long-range order in which the selenate rotations are partially correlated. This occurs at the incommensurate phase transition. However, the fact that the Raman spectra for the internal modes appear to be unaffected by the incommensurate phase transition suggests that the local disorder is basically unchanged by this transition.

Some further support, albeit indirect, for these ideas is provided by the work of de Pater[22] on the structure of "isomorphous" Rb_2ZnBr_4. From this work it appears that regions of incommensurate

structure are dynamically present in the high-temperature phase. In this structure the incommensurate displacements and distortions are significantly larger than in K_2SeO_4. Thus we expect the local order above T_i to be larger, and longer ranged. The existence of quasielastic scattering at the incommensurate wave vector in Rb_2ZnBr_4 above T_i and its apparent absence for K_2SeO_4 are consistent with these ideas.

The hypothesis of a "glassy" phase transition also offers a possible explanation of the observed DTA peaks. These, or at least the first near 400 K, can be accounted for by postulating that at these temperatures $kT \sim \Delta$. Thus, at higher temperatures the selenates become *dynamically* disordered between their respective double wells, undergoing thermally activated hopping between them. This change will not be detected by x-rays or any other probe that only examines the time- and space-averaged structure. Such a probe will still only "see" the structure as an ideal β-K_2SO_4 lattice. However, a probe such as Raman scattering, which effectively "sees" the instantaneous structure (this is so because individual scattering events take place on a time scale very much shorter than the jump time for selenate hopping), will continue to sense a noncentrosymmetric lattice. The defect-activated scattering, while still present, may change at the "glass transitions" since the qualitative nature of the responsible defects changes. It is also possible that the marked change in the low-frequency defect band observed at temperatures close to 400 K, where the first DTA peak occurs, could also be associated with these transitions.

The breadth of the observed DTA peaks is also consistent with our model: One does not expect losses of short-range order to occur suddenly as the temperature is increased. Thus there will be a broad peak in the specific heat.

The fact, discussed at some length earlier in this section, that only the Raman activity of the internal modes is strongly influenced by the apparent lack of a center of inversion symmetry is also made plausible by this model. These modes primarily involve intraselenate motions and their Raman activity is strongly influenced by the symmetry of the oxygen sublattice. Specifically, the gerade and ungerade classifications are only meaningful if *this sublattice* has strict inversion symmetry. If this is not so, as is the case for our model, then the selection rule which prohibits ungerade modes from Raman activity is broken and they will become visible.

There is, however, a most intriguing feature of all of the internal mode spectra: In each one the nine lines occur at nearly exactly the same frequencies—at least within the limits of the instrumental resolution. This is exactly what one would see if one were examining the scattering by an array of isolated selenate groups in a matrix such that each occupied a site of C_{2v} symmetry. In this case, all nine internal modes would have distinct frequencies; the degeneracies present for the free radical having been completely removed by the crystal field. Thus we are led to make an even stronger hypothesis: Not merely has the local distortion of the selenate sublattice removed the center of inversion symmetry, but the lack of long-range order has also "decoupled" the internal vibrations of the selenates so that these are localized (or quasilocalized) on the individual radicals. Then the four selenates in each unit cell instead of participating in 36 coupled vibrations, nine of which are active in each scattering geometry, vibrate independently at nine distinct frequencies each of which is the same for all four units and each of which is Raman active in all four geometries. The crucial point is that the possibility of phase coherence between the motions of pairs of selenates has been destroyed by the disorder. This picture is entirely consistent with our hypothesis of uncorrelated cantings of the selenate groups due to weak interselenate coupling. Moreover, this picture could also explain the observation, reported earlier, that if the scattering geometry is varied so that the polar (infrared-active) modes are excited first as purely "transverse" vibrations, and then as purely "longitudinal" vibrations, no frequency shifts are observed. If the vibrational excitations actually generated by Raman scattering are nonpropagating, then the distinctions "longitudinal" and "transverse" have no meaning and the observed frequencies *should not* change.

Finally, it should be noted that it is crucial to the present explanation that the selenate misorientations be small in order that all the selenates experience the same basic C_{2v} crystal field frequency splittings; otherwise one would observe not nine distinct sharp lines but four broad peaks. This requirement is entirely consistent with the x-ray data.

On the other hand, in the external vibrations, the selenates move much more as rigid units, and it can be argued that for these modes the overall motion is dictated by that of the potassium and selenium ions. Since these sublattices do possess inversion symmetry, the gerade-ungerade classification of vibrations remains valid and the selection rule which excludes ungerade vibrations from Raman activity remains in force.

Finally, with regard to the calculations in Ref. 1

which assumed that K_2SeO_4 had the ideal β-K_2SO_4 structure: These remain essentially valid for external modes for the following two reasons.

(a) The selenate rotations proposed by the present model are so small that their effect on the lattice-dynamical calculations for these modes would be correspondingly small.

(b) Since the proposed selenate rotations are both small and random, the only way to obtain a periodic structure on which to make a lattice-dynamical calculation is to place the oxygens at their average positions. The resultant force constants associated with bonds to oxygens in this periodic structure will then represent the averages of those in the real system. However, it is exactly these averages which will be sensed by those external vibrations studied experimentally. Specifically, the zero wave-vector optic vibrations, which involve uniform sublattice relative motions, sense average intersublattice force constants while vibrations propagating along the Σ ([100]) direction, which involve uniform relative displacements of neighboring planes within each sublattice, sense average interplanar force constants. Thus theory and experiment should be directly comparable.

In this section, we have proposed a general model that appears to accommodate most of our observations. However, we are not at present in a position to be specific as to its details: e.g., the axis of selenate rotation and the specific form of the double well potential. Also, the detailed nature of the "glassy phase" is unclear. The presence of at least one additional peak in the DTA data appears to indicate that there is more than one transition in this phase. Finally, we are implicitly postulating a connection between the proposed rotational disorder of the selenates and the incommensurate phase transition at 129 K. This despite the fact that we feel that the selenate canting is a basically "local" effect in that each selenate may be *inherently* unstable at the "ideal" orientation in the potential due to the static lattice. However, this basic instability may, at least in part, "drive" the incommensurate transition by weak interselenate coupling, ultimately favoring a cooperative lattice instability involving the whole lattice.

This picture has the attractive feature that it offers a possible explanation for the absence of soft-mode behavior above T_i in isomorphous materials, e.g., Rb_2ZnBr_4. One can argue as follows: In the ideal β-K_2SO_4 structure, such a material would show a cooperative soft-mode transition to the incommensurate phase. However, the $ZnBr_4$ tetrahedra are locally unstable in this structure; significantly more so than is the case for K_2SeO_4. Thus the canting tendency and coupling between different tetrahedral units are considerably stronger. Thus, even above T_i, they are strong enough to maintain the incommensurate structure on a local basis. What is lost above T_i is static long-range order. Thus in neutron or x-ray scattering, this transition will manifest itself by the appearance of an elastic peak at the incommensurate wave vector out of a diffuse elastic background, not by cooperative soft-mode behavior, as is observed. In the case of K_2SeO_4, the canting is much smaller and the interselenate coupling much weaker and cooperative soft-mode instability occurs.

V. SUMMARY OF CONCLUSIONS

K_2SeO_4 crystals, grown by slow evaporation of aqueous solutions, contain intrinsic defects that appear to be orientational disordering of the selenate groups in the selenate sublattice. This disorder destroys the center of symmetry that should be present in phase 2 although the crystal still appears centrosymmetric in x-ray structural studies because x-ray measurements average out the disorder while light scattering does not. A qualitative but detailed hypothetical model of the orientational disorder of the selenates has been offered that is consistent with the experimental results.

The modal analysis developed here differs in several respects from those given previously in the literature in which there have been both extra lines and missing lines that were not accounted for satisfactorily.

ACKNOWLEDGMENTS

This work was supported by the U. S. Army Research Office. The authors are indebted to Warren Lynn and Leo Klamath for the DTA measurements and to Professor Victor Day and Michael Frederich for the x-ray diffraction studies of the crystal structure.

[1]M. S. Haque and J. R. Hardy, Phys. Rev. B 21, 245 (1980).
[2]V. Fawcett, R. J. B. Hall, D. A. Long, and V. N. Sankaranarayanan, J. Raman Spectrosc. 2, 629 (1974); 3, 229 (1975).
[3]C. Caville, V. Fawcett, and D. A. Long, J. Raman Spectrosc. 7, 43 (1978).
[4]M. Wada, A. Sawada, Y. Ishibashi, Y. Takagai, and T. Sakudo, J. Phys. Soc. Jpn. 42, 1229 (1977); M. Wada, H. Uwe, A. Sawada, Y. Ishibashi, Y. Takagi, and T. Sakudo, *ibid.* 43, 544 (1977).
[5]M. Iizumi, J. D. Axe, G. Shirane, and K. Shimaoka, Phys. Rev. B 15, 4392 (1977).
[6]N. E. Massa, F. G. Ullman, and J. R. Hardy, Solid State Commun. 32, 1005 (1979).
[7]J. Petzelt, G. V. Kozlov, A. A. Volkov, and Y. Ishibashi, Z. Phys. B 33, 369 (1979).
[8]P. A. Fleury, S. Chiang, and K. B. Lyons, Solid State Commun. 31, 279 (1979).
[9]A. Escharri, M. Tello, and P. Gili, Solid State Commun. 36, 1021 (1980).
[10]B. N. Ganguly, F. G. Ullman, R. D. Kirby, and J. R. Hardy, Phys. Rev. B 13, 1344 (1976).
[11]R. D. Kirby and J. R. Duffey, Rev. Sci. Instrum. 50, 663 (1979).
[12]N. E. Massa, F. G. Ullman, and J. R. Hardy, Ferroelectrics 25, 601 (1980).
[13]W. L. Bragg, Proc. R. Soc. London Ser. A 105, 16 (1924).
[14]M. Frederich and V. Day (private communication).
[15]A. D. Prasad Rao, R. S. Katiyar, and S. P. S. Porto, in *Advances in Raman Spectroscopy,* edited by J. P. Mathieu (Heyden, London, 1973), Vol. 1, p. 174.
[16]A. F. Penna, A. Chaves, P. da R. Andrade, and S. P. S. Porto, Phys. Rev. B 13, 4907 (1976).
[17]G. Gattow, Acta Crystallogr. 15, 419 (1962).
[18]S. Shiozaki, A. Sawada, Y. Ishibashi, and Y. Takagi, J. Phys. Soc. Jpn. 43, 1314 (1977).
[19]A. Kálmán, J. S. Stephens, and D. W. J. Cruickshank, Acta Crystallogr. B 26, 1451 (1970).
[20]A. Balou, J. Nouet, A. W. Hewat, and F. J. Schafer, Ferroelectrics 25, 375 (1980).
[21]L. L. Boyer and J. R. Hardy, Phys. Rev. B 24, 2577 (1981).
[22]C. J. de Pater, Acta Crystallogr. B 35, 299 (1979).